JACS
JOURNAL OF THE AMERICAN CHEMICAL SOCIETY
pubs.acs.org/JACS
Article

Solid-Effect Dynamic Nuclear Polarization in Viscous Liquids at 9.4 T Using Narrow-Line Polarizing Agents

Andrei A. Kuzhelev,* Vasyl Denysenkov, Iram M. Ahmad, Olga Yu. Rogozhnikova, Dmitry V. Trukhin, Elena G. Bagryanskaya, Victor M. Tormyshev,* Snorri Th. Sigurdsson, and Thomas F. Prisner

Cite This: *J. Am. Chem. Soc.* 2023, 145, 10268−10274
Read Online

ABSTRACT: Dynamic nuclear polarization (DNP) is a hyperpolarization method that is widely used for increasing the sensitivity of nuclear magnetic resonance (NMR) experiments. DNP is efficient in solid-state and liquid-state NMR, but its implementation in the intermediate state, namely, viscous media, is still less explored. Here, we show that a ^{1}H DNP enhancement of over 50 can be obtained in viscous liquids at a magnetic field of 9.4 T and a temperature of 315 K. This was accomplished by using narrow-line polarizing agents in glycerol, both the water-soluble α,γ-bisdiphenylen-β-phenylallyl (BDPA) and triarylmethyl radicals, and a microwave/RF double-resonance probehead. We observed DNP enhancements with a field profile indicative of the solid effect and investigated the influence of microwave power, temperature, and concentration on the ^{1}H NMR results. To demonstrate potential applications of this new DNP approach for chemistry and biology, we show hyperpolarized ^{1}H NMR spectra of tripeptides, triglycine, and glypromate, in glycerol-d_8.

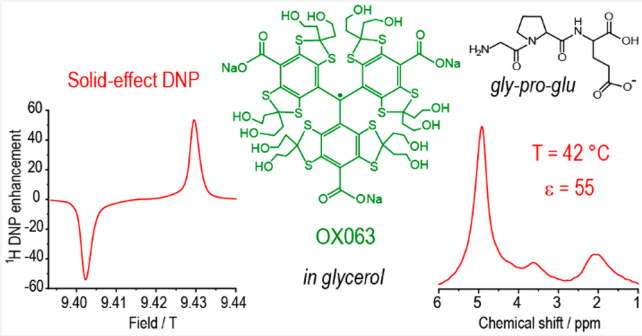

■ INTRODUCTION

Nuclear magnetic resonance (NMR) is a frequently used technique to determine the structure and dynamics of organic and inorganic molecules *in situ* and *in vivo*.[1,2] Nonetheless, the low interaction energy of nuclear spins with the external magnetic field leads to low spin polarization, which results in a low signal-to-noise ratio of NMR spectra. This limited sensitivity of NMR can be overcome by hyperpolarization methods that create strong nonequilibrium spin polarizations.[3] One such method is dynamic nuclear polarization (DNP),[4] in which electron spin polarization of paramagnetic molecules is transferred via resonant microwave excitation to the nuclear spins of the surrounding molecules. In the last decades, DNP has evolved, for both solid-[5] and liquid-state[6] NMR, to a powerful technique that has been used in numerous applications in biomolecular,[7−9] medical,[10] surface, and materials sciences.[11−15] In the solid state, four DNP mechanisms can be operational, namely, the Overhauser effect (OE),[16−18] the solid effect (SE),[19,20] the cross effect (CE),[21,22] and thermal mixing (TM).[23] In general, these mechanisms work best at a sample temperature of ≤100 K and can give large signal enhancements of ≥100 in the presence of carefully selected polarizing agents.[24,25] In liquids, only the OE mechanism is active, which requires the time-dependent interaction between electrons and nuclei on a time scale comparable with the reciprocal of the electron Larmor frequency ($1/\omega_e$). For this reason, the liquid-state OE is most effective at low magnetic field strength.[26−31] Nonetheless, it has been recently shown that the OE can yield significant ^{13}C ($\varepsilon \geq 600$)[32] and ^{31}P ($\varepsilon \geq 160$)[33] signal enhancements at magnetic fields of 9.4 and 14 T, respectively.

In viscous liquids, which exhibit molecular motion on the nanosecond to microsecond time scales, DNP enhancement can arise from both the OE and the SE. The SE is characterized by dipolar interaction between electron and nuclear spins and requires restricted motion, which is opposite to the OE. Several DNP studies have been performed for viscous liquids at low magnetic fields (0.33 T).[34−38] A sizable ^{1}H signal enhancement has been demonstrated in tetraethylene glycol,[34] polymers,[36] ionic liquids,[38] and crude oil.[37] With increasing sample viscosity, the crossover from OE to SE DNP can be studied; for example, poly(butadiene-1,4) had a maximum ^{1}H enhancement of ∼−1 by OE and ∼10 by SE using α,γ-bisdiphenylene-β-phenylallyl (BDPA) as a polarizing agent.[36] Recently, we reported unexpected solid-like high-field DNP in the fluid phase of lipid bilayers using BDPA radicals.[39] The ^{1}H DNP enhancement of up to ±12 was obtained for the

Received: February 6, 2023
Published: April 27, 2023

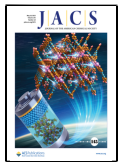

https://doi.org/10.1021/jacs.3c01358
J. Am. Chem. Soc. 2023, 145, 10268−10274

SE mechanism at a temperature of ∼320 K and a magnetic field of 9.4 T.

In this study, we demonstrate up to ±45-fold ^{1}H signal enhancement by SE DNP in glycerol at a temperature of ∼315 K and a magnetic field of 9.4 T. We used two classes of narrow EPR line polarizing agents, a water-soluble BDPA (ws-BDPA) and triarylmethyl radicals (Finland and OX063, see Figure 1) at concentrations of 10−100 mM. We show that ^{1}H SE DNP can be used to study a tripeptide, triglycine and glypromate, with the highest enhancement value of ∼55 using 25 mM of OX063 as a polarizing agent.

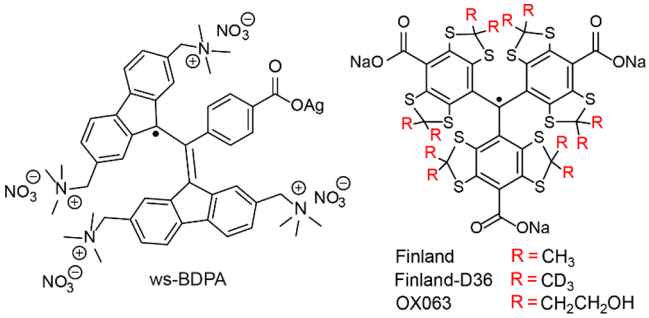

Figure 1. Structure of the radicals used in this study: a water-soluble BDPA radical and various triarylmethyl radicals.

■ EXPERIMENTAL SECTION

Water-soluble BDPA,[40] Finland,[41] Finland-D36,[42] and OX063[42] were synthesized according to literature protocols. Glycerol, glycerol-d_8 (98% atom D), triglycine (gly-gly-gly), and glypromate (gly-pro-glu) were obtained from Sigma-Aldrich. The concentration of the radicals was in the range from 10 to 100 mM and was determined by X-band CW EPR at room temperature (Figure S2). A solution of a tripeptide (triglycine and glypromate), in glycerol-d_8, doped with 25 mM OX063, was prepared as follows: the tripeptides were dissolved in sodium deuteroxide solution (40 wt % in D_2O) with a 1:1 molar ratio (tripeptide:NaOD) and subsequently diluted in glycerol-d_8 to a peptide concentration of 2 M. Finally, OX063 was added to the solution as a solid.

^{1}H DNP and CW EPR were performed on a home-built DNP spectrometer, a modified Bruker Avance II wide-bore spectrometer operating at 9.4 T.[43] Microwaves were generated by a 12 W gyrotron (Gycom, Russian Federation) operating at 264 GHz. The DNP probe is a home-built Fabry−Perot/stripline double-resonance structure (260 GHz/400 MHz).[44] DNP enhanced and reference (MW off) NMR FID signals were recorded with a standard 90° RF-pulse excitation. The 90° pulse length was 25 μs, and the repetition time was optimized for each ^{1}H NMR/DNP experiments and set to 1 s for each measurement. The DNP enhancement was measured by integration of all protons of the glycerol with and without microwave irradiation. The enhancement was then calculated according to $\varepsilon = (I/I_0) - 1$, where I and I_0 are the dynamic and the Boltzmann nuclear polarizations, respectively.

J-band CW EPR measurements were carried out at 315 K with the following parameters: microwave frequency 264 GHz, microwave power 5 mW, sweep width 44 mT, field modulation frequency 5 kHz, field modulation amplitude 0.2 mT, time constant 0.1 s, number of points 1101, and number of scans 1.

^{1}H NMR spectra of tripeptides in deuterated water (C = 0.1 M) and in glycerol-d_8 (C = 2 M) were measured at room temperature using a commercial Bruker BBI probehead.

■ RESULTS

We recently demonstrated that BDPA radicals can be used to polarize lipid bilayers in the fluid phase through the SE mechanism at high magnetic fields.[39] The lipid bilayers represent an example of a viscous medium, where molecular motion is on the nanosecond to microsecond time scale. To find out if the DNP mechanism is also operational in other viscous liquids, we studied glycerol doped with polarizing agents that have a narrow EPR line and thus can effectively drive forbidden electron−nuclear spin transitions. We investigated two classes of polarizing agents, BDPA and triarylmethyl radicals, that are often used for SE DNP in the solid state.[25] It has been shown that BDPA has limited persistence,[45] but tetraalkylammonium BDPA salts have improved stability;[40] we used one such derivative in this work (ws-BDPA, Figure 1). We also studied three trityl derivatives, Finland, Finland-D36, and OX063 (Figure 1). The variety of these radicals allowed us to investigate the SE mechanism, with respect to both the type of radical (BDPA and triarylmethyl) and the molecular weight (749, 997, 1357 g/mol for ws-BDPA, Finland, and OX063, respectively), as well as on the deuteration of the radical (Finland and Finland-D36).

CW EPR Spectra. The EPR spectra of the ws-BDPA and trityl radicals in glycerol were recorded at X-band (9 GHz) (Figure S2) and J-band (260 GHz) (Figure 2) frequencies.

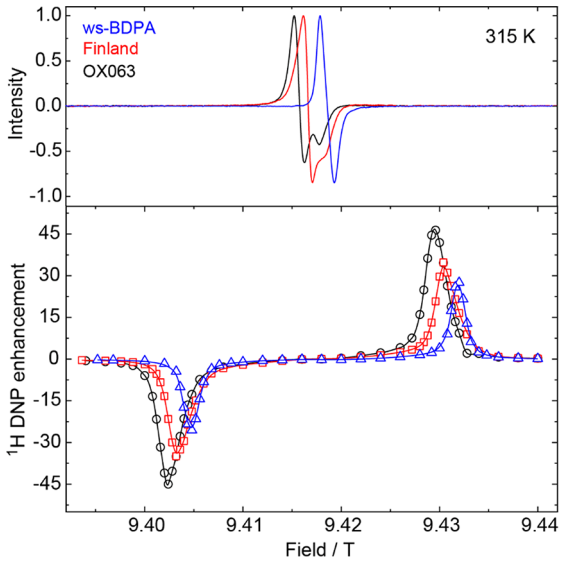

Figure 2. J-band CW EPR spectra (upper) of ws-BDPA, Finland, and OX063 radicals in glycerol (100 mM) and field profile of the ^{1}H DNP enhancement for all protons of the glycerol (lower) at a temperature of 315 K. The antisymmetric peaks are located at magnetic field strengths displaced by $\pm\omega_H/\gamma_e$ compared to the EPR resonance field positions, suggesting that the DNP mechanism is a solid effect.

The upper trace in Figure 2 shows the J-band EPR spectra for ws-BDPA, Finland, and OX063 at a concentration of 100 mM and a sample temperature of 315 K. The EPR spectrum of ws-BDPA revealed a symmetric narrow EPR line, whereas asymmetric EPR lines were observed for the trityl radicals, presumably due to the anisotropy of the trityl g-tensor, which results in a weakly pronounced shoulder at the high field edge of the spectrum. The shift of the EPR spectra for these radicals can be explained by different g-tensors (g_x = 2.00276, g_y = 2.00273, g_z = 2.00250 for ws-BDPA, g_x = 2.00336, g_y = 2.00305, g_z = 2.00263 for Finland, and g_x = 2.00331, g_y = 2.00316, g_z = 2.00280 for OX063, see Figure S5). The anisotropy of the trityl g-tensor is too small to extract

https://doi.org/10.1021/jacs.3c01358
J. Am. Chem. Soc. 2023, 145, 10268−10274

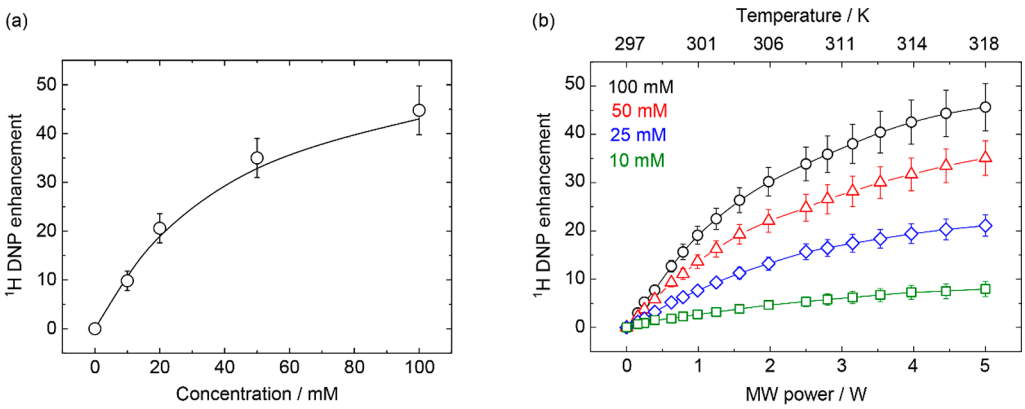

Figure 3. ^{1}H DNP enhancement for OX063 in glycerol (a) as a function of the concentration, measured at 315 K, and (b) as a function of the applied microwave power and sample temperature (for temperature calibration see Figure S8) for different radical concentrations: 100 mM (black, ○), 50 mM (red, Δ), 25 mM (blue, ◊), 10 mM (green, □). The DNP enhancement was measured at a magnetic field corresponding to the high-field SE position. Analogous information for the other radicals is provided in the SI.

information about the rotational correlation time. Nevertheless, it has become possible for modified radicals, such as a Finland trityl bearing a ^{13}C label on the central carbon atom[46] (Finland-$^{13}C_1$, see SI). For the $^{13}C_1$-labeled Finland radical in glycerol, the CW EPR spectrum exhibits an anisotropic immobilized line shape in the temperature range of 300−325 K at X-band frequency (Figure S3). The fitting of EPR spectra with the ^{13}C hyperfine tensor of $A_x = A_y = 17$ MHz and $A_z = 165$ MHz shows that the rotational correlation time of Finland-$^{13}C_1$ trityl ranges from 78 ± 8 ns at 300 K up to 21 ± 3 ns at 325 K.

^{1}H DNP Field Profile. The ^{1}H DNP field profile of the glycerol protons is antisymmetric with respect to the radical EPR resonance position (Figure 2, lower). The peaks are located at magnetic field strengths displaced by $\pm\omega_H/\gamma_e$, compared to the corresponding EPR resonance field position that is characteristic for the SE mechanism. The DNP peaks for ws-BDPA are symmetric, but slightly asymmetric for the trityl radicals, similar to what was observed in the EPR spectra. The width of the DNP peaks is narrower for BDPA, compared to the trityl radicals, as seen in the DNP field profile, normalized to the maximum amplitude of the high-field peak (Figure S4). The width and the shift of the DNP field profiles for the different polarizing agents are in good agreement with the EPR line width and *g*-factor of the corresponding radical. The maximum ^{1}H DNP enhancement increases in the order BDPA ($\varepsilon = \pm 26$), Finland ($\varepsilon = \pm 35$), OX063 ($\varepsilon = \pm 45$). Note that for the fully deuterated Finland trityl (Finland-D36), we obtain a similar ^{1}H DNP enhancement to that with the protonated analogue ($\varepsilon = \pm 33$, Figure S10), within the measurement error of 10%.

Concentration Dependence of SE. Figure 3a shows the maximum ^{1}H DNP enhancements at a microwave power of ∼5 W for different concentrations of OX063 radicals; the data for the other radicals are shown in Figure S6. With increasing concentration of the polarizing agent, the ^{1}H DNP enhancements increase. However, at higher radical concentrations (≥50 mM) the NMR line width becomes broader (Figure S7). Thus, the optimum concentration of the polarizing agent is ∼25 mM, leading to a large DNP enhancement and minimal effect on the NMR line width.

Microwave Power Dependence of SE. Figure 3b shows the ^{1}H DNP enhancement at the high-field SE position as a function of the applied microwave power and the temperature, because the microwave excitation leads to sample heating. We calibrated the sample temperature using glycerol as a "chemical shift thermometer", similar to what has been described for ethylene glycol.[47] In glycerol, the relative chemical shift of the OH and the CH/CH_2 peaks exhibits a strong temperature dependence, which can be calibrated (Figure S8). Changing the applied microwave power from 0 to 5 W, the sample temperature increased from 296 K to ∼320 K. Usually for SE polarization transfer, DNP enhancement increases almost linearly with increasing microwave power, due to the inability to saturate forbidden electron−nuclear spin transitions.[25] However, we observed a nonlinear increase of SE enhancement (Figure 3 and Figure S9). The deviation from linearity can be explained by the temperature increase, which results in an exponential decline of glycerol viscosity (Figure S11). Indeed, the temperature dependence of ^{1}H DNP enhancement, measured at a fixed microwave power, demonstrates a monotonic decrease (Figure S12). Thus, at lower viscosity of glycerol, the anisotropic hyperfine interaction between the electron and glycerol proton spins is partly averaged out, resulting in a decrease of SE efficiency and, hence, reduction of the DNP enhancement factor.

^{1}H DNP NMR of Tripeptides. To demonstrate the applicability of DNP NMR in viscous solutions, we recorded NMR spectra of the sodium salt of two tripeptides, namely, triglycine (gly-gly-gly) and glypromate (gly-pro-glu), in glycerol-d_8 at a magnetic field of 9.4 T. However, we first measured the ^{1}H NMR spectra using a standard Bruker BBI probehead in D_2O to identify the proton peaks (Figure 4d). A significant broadening of the NMR lines appeared when changing the solvent from water to glycerol (Figure 4c), due to slowing down the molecular motion of molecules. Using a Fabry−Pérot/stripline resonator, we obtained broader NMR lines, compared to the Bruker probehead (Figure 4b). However, it was still possible to distinguish the different protons of the tripeptides. We used 25 mM OX063 radical as a polarizing agent, which gave the highest SE enhancement factor in glycerol, relative to the other radicals. The addition of polarizing agents to the solution leads to further slight broadening of the NMR lines (Figure 4a,b); however, it results only in 30% loss of signal intensity (Figure S14). The observed enhancement factors were ∼35 for triglycine and ∼55 for glypromate. Note that for glycerol we obtained lower enhancement (about 20).

https://doi.org/10.1021/jacs.3c01358
J. Am. Chem. Soc. 2023, 145, 10268−10274

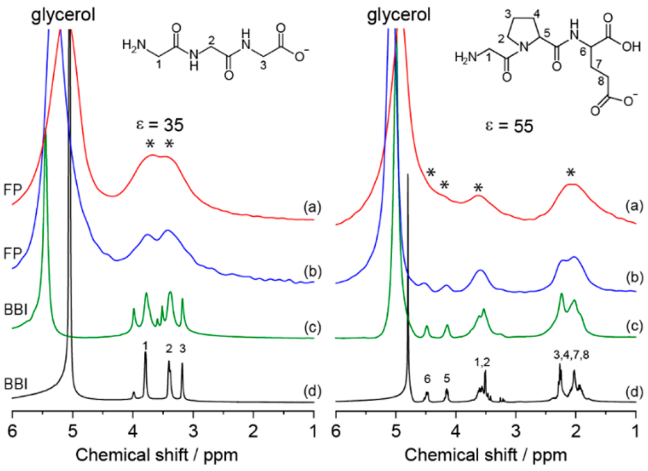

Figure 4. (a) ^{1}H DNP spectra for tripeptide (2 M) in glycerol-d_8, containing 25 mM OX063, at 9.4 T, MW power of 5 W, and a sample temperature of ∼315 K; (b) ^{1}H NMR spectra for 2 M tripeptide in glycerol-d_8 using a Fabry−Perot/stripline probehead (FP); (c) ^{1}H NMR spectra for tripeptide (2 M) in glycerol-d_8 using a Bruker BBI probehead; (d) ^{1}H NMR spectrum for tripeptide (0.1 M) in D_2O using the Bruker BBI probehead. Left and right figures show the results for triglycine (gly-gly-gly) and glypromate (gly-pro-glu), respectively. Because of the high sensitivity of the chemical shift, for ^{1}H peaks of triglycine to pH and solvent,[48] the ^{1}H triglycine peaks in glycerol are slightly different than in water. Stars show hyperpolarized ^{1}H peaks with ε = 35 and ε = 55 for triglycine and glypromate, respectively. Spectra were recorded at the high-field SE position.

■ DISCUSSION

Our near-physiological temperature DNP experiments in a magnetic field of 9.4 T clearly revealed that only one mechanism was operational in polarization transfer, namely, the SE. It should be noted that the negative OE in the middle of the field profile was absent, but usually the OE is much less efficient at high magnetic fields for bulky polarizing agents and viscous liquids.[49] The SE mechanism was confirmed by both the displacement of both positive and negative peaks in the DNP field profile by $\pm\omega_H/\gamma_e$, compared to the EPR resonance position, and the similar widths of the peaks in the DNP field profile and the EPR spectra of the polarizing agents. The SE mechanism is based on the excitation of forbidden zero-quantum and double-quantum transitions in a coupled electron−nuclear spin system. These transitions are possible if (i) the anisotropic part of the hyperfine interaction between the electron spin of the polarizing agent and the nuclear spin of the target molecule is large enough, (ii) the molecular motions are restricted or slow enough to avoid averaging out the anisotropic hyperfine interaction, (iii) the individual EPR line of the polarizing agent is sufficiently narrow, and (iv) a large microwave B_1 field is applied. The latter condition was achieved with our home-built DNP setup, which is equipped with a microwave/RF resonant Fabry−Pérot/stripline probehead and with a gyrotron as the microwave source, having a maximum power of ∼5 W. This DNP setup allows us to very efficiently drive the forbidden electron−nuclear spin transitions.

We investigated two different classes of polarizing agent, BDPA and triarylmethyl radicals. These polarizing agents are carbon-centered radicals that have a very small g-anisotropy and, hence, a very narrow EPR line width. These two types of radicals differ from each other mainly in how the unpaired electron spin density is delocalized and shielded. Triarylmethyl radicals carry most of the electron spin density on the central carbon, which is sterically shielded by the sulfur substituents on the aromatic rings and is completely isolated from the surrounding molecules.[50] In contrast, the electron spin density of the BDPA radicals is delocalized on the fluorene moieties, which are not shielded from solvents. Despite these differences in their chemical structures, both radicals are very promising polarizing agents for SE DNP in viscous liquids, mostly due to their narrow EPR line width and slow molecular motion.

In the SE mechanism, the molecular motion has two main functions. On one hand it averages out the anisotropic hyperfine interaction between the electron and nuclear spins, and on the other hand propagates the polarization to other solvent molecules. In viscous solutions, in which the molecular motion is restricted, the small residuals of the incompletely averaged dipolar interaction allow nuclear polarization. The correlation time, τ_c, the characteristic time of the dynamic process of the SE mechanism, can be described by $\tau_c^{-1} = \tau_{R1}^{-1} + \tau_{R2}^{-1} + \tau_{e1}^{-1} + \tau_{e2}^{-1}$ where τ_{R1} and τ_{R2} are the rotational correlation times of the polarizing agent and the molecule to be polarized, respectively, and τ_{e1} and τ_{e2} are the longitudinal and transverse electron spin relaxation times of the radical, respectively. Note that the lifetime of the radical−solvent complex can be ignored, because the dynamic polarization is quickly produced in each nuclear spin by its dipolar interaction with the electron spin.[51] In a glycerol solution, the radicals have a rotational correlation time τ_R of several tens of nanoseconds at a temperature chosen for our DNP measurements (T = 315 K), as demonstrated for the Finland-$^{13}C_1$ radical by X-band EPR (τ_R = 37 ns, Figure S3). Under the same conditions, the rotational correlation times of the analytes and the electron spin relaxation time of the radical at a J-band frequency are also in the nanosecond time range. Therefore, neither τ_R or τ_e can be neglected for characterizing the molecular motion in viscous liquids. Describing the SE mechanism in viscous systems is more complicated and requires further investigation.

We observed an increase in the ^{1}H SE DNP enhancement for the polarizing agents in the order ws-BDPA (ε = 26 ± 3), Finland (ε = 35 ± 4), OX063 (ε = 45 ± 5) when using a 100 mM concentration of the polarizing agents in glycerol. The analytes also showed different enhancement under identical DNP conditions (25 mM OX063 in glycerol): glycerol (ε = 20 ± 2), triglycine (ε = 35 ± 4), and glypromate (ε = 55 ± 6). These differences in the ^{1}H SE DNP enhancements can be explained by the different anisotropic hyperfine interaction between the polarizing agent and the analytes and by slower molecular motion (namely, increasing correlation time τ_c) with increasing molecular weight of either the polarizing agent or the analyte. If we assume that the anisotropic hyperfine interaction is very similar for various polarizing agents in different viscous systems, the dependence of ^{1}H SE DNP enhancement on the molecular weight of (i) the polarizing agent and (ii) the analytes (glycerol and tripeptides) should correlate. Indeed, when we plot the DNP enhancement as a function of the molecular weight, we obtained a linear increase of ^{1}H SE DNP enhancement with increase of the molecular weight of either the polarizing agent or the analyte (Figure S13). This strongly suggests that the SE mechanism strongly depends on the correlation time τ_c and, hence, the molecular size of the radical and the target molecule. This observation provides a guideline for further development of improved

https://doi.org/10.1021/jacs.3c01358
J. Am. Chem. Soc. 2023, 145, 10268−10274

polarizing agents and approaches for studying large biological complexes at physiological temperatures using SE DNP.

Based on our results, we propose the following polarization pathway for the SE mechanism in viscous liquids. The first step is the direct transfer of polarization from the electron spin of the polarizing agent to the nearest nuclei of the analyte, as confirmed by lack of (i) dependence on the nature of the radical (BDPA vs triarylmethyl) and (ii) dependence on deuteration of the triarylmethyl radicals (Finland vs Finland-D36). Further propagation of the polarization to other solvent or tripeptides molecules can be accomplished by molecular diffusion of the polarized molecules. Indeed, the rotational and translational correlation times of glycerol are a few nanoseconds under our DNP condition,[52] and, therefore, the sample behaves as a liquid on the time scale of the NMR relaxation time (a few hundreds of milliseconds, see Table S1). This results in a very fast overall polarization time of the sample, determined by the proton T_1 time (see SI), allowing a fast repetition of the experiment.

■ CONCLUSIONS

In conclusion, we have demonstrated a versatile approach for obtaining large ^{1}H hyperpolarization in viscous liquids generated by the SE mechanism for a series of polarizing agents that are derivatives of BDPA and triarylmethyl radicals. Up to 20- and 55-fold increases in signal intensity were achieved for glycerol and a tripeptide (gly-pro-glu) in glycerol-d_8 doped with 25 mM OX063, respectively. Qualitative interpretation of the data shows that the SE DNP enhancements are strongly affected by the hyperfine coupling strength, which is partly motionally averaged. To our knowledge, this is the largest ^{1}H DNP enhancement by the SE mechanism in a viscous system at a magnetic field of 9.4 T and near-physiological temperatures. These promising DNP results could potentially be interesting for a study of viscous liquids at high magnetic fields and ambient temperatures in biomolecular and material sciences.

■ ASSOCIATED CONTENT

Supporting Information

The Supporting Information is available free of charge at https://pubs.acs.org/doi/10.1021/jacs.3c01358.

More details on the synthesis of radicals, the additional EPR, NMR, and DNP data, and calculations (PDF)

■ AUTHOR INFORMATION

Corresponding Authors

Andrei A. Kuzhelev − *Institute of Physical and Theoretical Chemistry and Center for Biomolecular Magnetic Resonance, Goethe University Frankfurt am Main, 60438 Frankfurt am Main, Germany;* orcid.org/0000-0003-3445-2921; Email: kuzhelev@chemie.uni-frankfurt.de

Victor M. Tormyshev − *N. N. Vorozhtsov Institute of Organic Chemistry, Siberian Branch of Russian Academy of Sciences (SB RAS), 630090 Novosibirsk, Russia*; Email: torm@nioch.nsc.ru

Authors

Vasyl Denysenkov − *Institute of Physical and Theoretical Chemistry and Center for Biomolecular Magnetic Resonance, Goethe University Frankfurt am Main, 60438 Frankfurt am Main, Germany*

Iram M. Ahmad − *Department of Chemistry, Science Institute, University of Iceland, 107 Reykjavik, Iceland*

Olga Yu. Rogozhnikova − *N. N. Vorozhtsov Institute of Organic Chemistry, Siberian Branch of Russian Academy of Sciences (SB RAS), 630090 Novosibirsk, Russia*

Dmitry V. Trukhin − *N. N. Vorozhtsov Institute of Organic Chemistry, Siberian Branch of Russian Academy of Sciences (SB RAS), 630090 Novosibirsk, Russia*

Elena G. Bagryanskaya − *N. N. Vorozhtsov Institute of Organic Chemistry, Siberian Branch of Russian Academy of Sciences (SB RAS), 630090 Novosibirsk, Russia;* orcid.org/0000-0003-0057-383X

Snorri Th. Sigurdsson − *Department of Chemistry, Science Institute, University of Iceland, 107 Reykjavik, Iceland;* orcid.org/0000-0003-2492-1456

Thomas F. Prisner − *Institute of Physical and Theoretical Chemistry and Center for Biomolecular Magnetic Resonance, Goethe University Frankfurt am Main, 60438 Frankfurt am Main, Germany;* orcid.org/0000-0003-2850-9573

Complete contact information is available at: https://pubs.acs.org/10.1021/jacs.3c01358

Notes

The authors declare no competing financial interest.

■ ACKNOWLEDGMENTS

A.A.K. acknowledges the DFG (Deutsche Forschungsgemeinschaft, Grant No. 518679424) and FOCUS program funded by Goethe University of Frankfurt for financial support of this project. V.M.T. acknowledges the Russian Science Foundation (project number 21-14-00219) for financial support of trityl syntheses. A.A.K., V.D., and T.F.P. acknowledge the Center for Biomolecular Magnetic Resonance for financial support.

■ ABBREVIATIONS

NMR, nuclear magnetic resonance; DNP, dynamic nuclear polarization; OE, Overhauser effect; SE, solid effect; CE, cross effect; TM, thermal mixing; BDPA, α,γ-bisdiphenylene-β-phenylallyl

■ REFERENCES

(1) Blasco, T. Insights into Reaction Mechanisms in Heterogeneous Catalysis Revealed by in Situ NMR Spectroscopy. *Chem. Soc. Rev.* **2010**, *39* (12), 4685−4702.

(2) Malet-Martino, M.; Holzgrabe, U. NMR Techniques in Biomedical and Pharmaceutical Analysis. *J. Pharm. Biomed. Anal.* **2011**, *55* (1), 1−15.

(3) Eills, J.; Budker, D.; Cavagnero, S.; Chekmenev, E. Y.; Elliott, S. J.; Jannin, S.; Lesage, A.; Matysik, J.; Meersmann, T.; Prisner, T.; Reimer, J. A.; Yang, H.; Koptyug, I. V. Spin Hyperpolarization in Modern Magnetic Resonance. *Chem. Rev.* **2023**, *123* (4), 1417−1551.

(4) Ni, Q. Z.; Daviso, E.; Can, T. V.; Markhasin, E.; Jawla, S. K.; Swager, T. M.; Temkin, R. J.; Herzfeld, J.; Griffin, R. G. High Frequency Dynamic Nuclear Polarization. *Acc. Chem. Res.* **2013**, *46* (9), 1933−1941.

(5) Griffin, R. G.; Swager, T. M.; Temkin, R. J. High Frequency Dynamic Nuclear Polarization: New Directions for the 21st Century. *J. Magn. Reson.* **2019**, *306*, 128−133.

(6) Denysenkov, V. P.; Prisner, T. F. Liquid-State Overhauser DNP at High Magnetic Fields. *eMagRes.* **2019**, *8* (1), 41−54.

(7) Su, Y.; Andreas, L.; Griffin, R. G. Magic Angle Spinning NMR of Proteins: High-Frequency Dynamic Nuclear Polarization and 1H Detection. *Annu. Rev. Biochem.* **2015**, *84*, 465−497.

(8) Kaplan, M.; Cukkemane, A.; Van Zundert, G. C. P.; Narasimhan, S.; Daniëls, M.; Mance, D.; Waksman, G.; Bonvin, A. M. J. J.; Fronzes, R.; Folkers, G. E.; Baldus, M. Probing a Cell-Embedded Megadalton Protein Complex by DNP-Supported Solid-State NMR. *Nat. Methods* **2015**, *12* (7), 649−652.
(9) Mao, J.; Aladin, V.; Jin, X.; Leeder, A. J.; Brown, L. J.; Brown, R. C. D.; He, X.; Corzilius, B.; Glaubitz, C. Exploring Protein Structures by DNP-Enhanced Methyl Solid-State NMR Spectroscopy. *J. Am. Chem. Soc.* **2019**, *141* (50), 19888−19901.
(10) Ardenkjær-Larsen, J. H.; Golman, K.; Gram, A.; Lerche, M. H.; Servin, R.; Thaning, M.; Wolber, J. Increase of Signal-to-Noise of More than 10,000 Times in Liquid State NMR. *Proc. Natl. Acad. Sci. U. S. A.* **2003**, *100* (18), 10158−10163.
(11) Rossini, A. J.; Zagdoun, A.; Lelli, M.; Lesage, A.; Copéret, C.; Emsley, L. Dynamic Nuclear Polarization Surface Enhanced NMR Spectroscopy. *Acc. Chem. Res.* **2013**, *46* (9), 1942−1951.
(12) Kobayashi, T.; Perras, F. A.; Slowing, I. I.; Sadow, A. D.; Pruski, M. Dynamic Nuclear Polarization Solid-State NMR in Heterogeneous Catalysis Research. *ACS Catal.* **2015**, *5* (12), 7055−7062.
(13) Thankamony, A. S. L.; Knoche, S.; Bothe, S.; Drochner, A.; Jagtap, A. P.; Sigurdsson, S. T.; Vogel, H.; Etzold, B. J. M.; Gutmann, T.; Buntkowsky, G. Characterization of V-Mo-W Mixed Oxide Catalyst Surface Species by 51V Solid-State Dynamic Nuclear Polarization NMR. *J. Phys. Chem. C* **2017**, *121* (38), 20857−20864.
(14) Wolf, T.; Kumar, S.; Singh, H.; Chakrabarty, T.; Aussenac, F.; Frenkel, A. I.; Major, D. T.; Leskes, M. Endogenous Dynamic Nuclear Polarization for Natural Abundance 17O and Lithium NMR in the Bulk of Inorganic Solids. *J. Am. Chem. Soc.* **2019**, *141* (1), 451−462.
(15) Moroz, I. B.; Leskes, M. Dynamic Nuclear Polarization Solid-State NMR Spectroscopy for Materials Research. *Annu. Rev. Mater. Res.* **2022**, *52*, 25−55.
(16) Overhauser, A. W. Polarization of Nuclei in Metals. *Phys. Rev.* **1953**, *92* (2), 411−415.
(17) Carver, T. R.; Slichter, C. P. Polarization of Nuclear Spins in Metals. *Phys. Rev.* **1953**, *92* (1), 212−213.
(18) Carver, T. R.; Slichter, C. P. Experimental Verification of the Overhauser Nuclear Polarization Effect. *Phys. Rev.* **1956**, *102* (4), 975−980.
(19) Jeffries, C. D. Polarization of Nuclei by Resonance Saturation in Paramagnetic Crystals. *Phys. Rev.* **1957**, *106* (1), 164−165.
(20) Abragam, A.; Proctor, W. G. Une Nouvelle Methode de Polarisation Dynamique Des Noyaux Atomiques Dans Les Solides. *C. R. Hebd. Seances Acad. Sci.* **1958**, *246* (15), 2253−2256.
(21) Kessenikh, A.; Lushchikov, V.; Manenkov, A.; Taran, Y. Proton Polarization in Irradiated Polyethylenes. *Sov. Phys.-Solid State* **1963**, *5*, 321−329.
(22) Hwang, C. F.; Hill, D. A. Phenomenological Model for the New Effect in Dynamic Polarization. *Phys. Rev. Lett.* **1967**, *19* (18), 1011.
(23) Abragam, A.; Goldman, M. Principles of Dynamic Nuclear Polarisation. *Rep. Prog. Phys.* **1978**, *41* (3), 395−467.
(24) Casano, G.; Karoui, H.; Ouari, O. Polarizing Agents: Evolution and Outlook in Free Radical Development for DNP. *eMagRes.* **2018**, *7* (4), 195−208.
(25) Biedenbänder, T.; Aladin, V.; Saeidpour, S.; Corzilius, B. Dynamic Nuclear Polarization for Sensitivity Enhancement in Biomolecular Solid-State NMR. *Chem. Rev.* **2022**, *122* (10), 9738−9794.
(26) Liu, G.; Levien, M.; Karschin, N.; Parigi, G.; Luchinat, C.; Bennati, M. One-Thousand-Fold Enhancement of High Field Liquid Nuclear Magnetic Resonance Signals at Room Temperature. *Nat. Chem.* **2017**, *9* (7), 676−680.
(27) Van Der Heijden, G. H. A.; Kentgens, A. P. M.; Van Bentum, P. J. M. Liquid State Dynamic Nuclear Polarization of Ethanol at 3.4 T (95 GHz). *Phys. Chem. Chem. Phys.* **2014**, *16* (18), 8493−8502.
(28) Barnes, R.; Sun, S.; Fichou, Y.; Dahlquist, F. W.; Heyden, M.; Han, S. Spatially Heterogeneous Surface Water Diffusivity around Structured Protein Surfaces at Equilibrium. *J. Am. Chem. Soc.* **2017**, *139* (49), 17890−17901.
(29) Banerjee, A.; Dey, A.; Chandrakumar, N. Slow Molecular Motions in Ionic Liquids Probed by Cross-Relaxation of Nuclear Spins during Overhauser Dynamic Nuclear Polarization. *Angew. Chemie - Int. Ed.* **2016**, *55* (47), 14756−14761.
(30) Garcia, S.; Walton, J. H.; Armstrong, B.; Han, S.; McCarthy, M. J. L-Band Overhauser Dynamic Nuclear Polarization. *J. Magn. Reson.* **2010**, *203* (1), 138−143.
(31) Fehling, P.; Buckenmaier, K.; Dobrynin, S. A.; Morozov, D. A.; Polienko, Y. F.; Khoroshunova, Y. V.; Borozdina, Y.; Mayer, P.; Engelmann, J.; Scheffler, K.; Angelovski, G.; Kirilyuk, I. A. The Effects of Nitroxide Structure upon 1H Overhauser Dynamic Nuclear Polarization Efficacy at Ultralow-Field. *J. Chem. Phys.* **2021**, *155* (14), 1ENG.
(32) Orlando, T.; Dervişoğlu, R.; Levien, M.; Tkach, I.; Prisner, T. F.; Andreas, L. B.; Denysenkov, V. P.; Bennati, M. Dynamic Nuclear Polarization of 13C Nuclei in the Liquid State over a 10 T Field Range. *Angew. Chemie - Int. Ed.* **2019**, *58* (5), 1402−1406.
(33) Dubroca, T.; Smith, A. N.; Pike, K. J.; Froud, S.; Wylde, R.; Trociewitz, B.; McKay, J.; Mentink-Vigier, F.; van Tol, J.; Wi, S.; Brey, W.; Long, J. R.; Frydman, L.; Hill, S. A Quasi-Optical and Corrugated Waveguide Microwave Transmission System for Simultaneous Dynamic Nuclear Polarization NMR on Two Separate 14.1 T Spectrometers. *J. Magn. Reson.* **2018**, *289*, 35−44.
(34) Leblond, J.; Uebersfeld, J.; Korringa, J. Study of the Liquid-State Dynamics by Means of Magnetic Resonance and Dynamic Polarization. *Phys. Rev. A* **1971**, *4* (4), 1532−1539.
(35) Karyagin, V. V.; Dovgopol, S. P. Frequency Dependence of Dynamic Nuclear Polarization in Viscous Solutions. *Sov. Phys. J.* **1972**, *15* (1), 54−57.
(36) Neudert, O.; Reh, M.; Spiess, H. W.; Münnemann, K. X-Band DNP Hyperpolarization of Viscous Liquids and Polymer Melts. *Macromol. Rapid Commun.* **2015**, *36* (10), 885−889.
(37) Gizatullin, B.; Gafurov, M.; Vakhin, A.; Rodionov, A.; Mamin, G.; Orlinskii, S.; Mattea, C.; Stapf, S. Native Vanadyl Complexes in Crude Oil as Polarizing Agents for in Situ Proton Dynamic Nuclear Polarization. *Energy Fuels* **2019**, *33* (11), 10923−10932.
(38) Gizatullin, B.; Mattea, C.; Stapf, S. Molecular Dynamics in Ionic Liquid/Radical Systems. *J. Phys. Chem. B* **2021**, *125* (18), 4850−4862.
(39) Kuzhelev, A. A.; Dai, D.; Denysenkov, V.; Prisner, T. F. Solid-like Dynamic Nuclear Polarization Observed in the Fluid Phase of Lipid Bilayers at 9.4 T. *J. Am. Chem. Soc.* **2022**, *144* (3), 1164−1168.
(40) Mandal, S.; Sigurdsson, S. T. Water-Soluble BDPA Radicals with Improved Persistence. *Chem. Commun.* **2020**, *56* (86), 13121−13124.
(41) Rogozhnikova, O. Y.; Vasiliev, V. G.; Troitskaya, T. I.; Trukhin, D. V.; Mikhalina, T. V.; Halpern, H. J.; Tormyshev, V. M. Generation of Trityl Radicals by Nucleophilic Quenching of Tris(2,3,5,6-Tetrathiaaryl)Methyl Cations and Practical and Convenient Large-Scale Synthesis of Persistent Tris(4-Carboxy-2,3,5,6-Tetrathiaaryl)-Methyl Radical. *Eur. J. Org. Chem.* **2013**, *2013* (16), 3347−3355.
(42) Kuzhelev, A. A.; Trukhin, D. V.; Krumkacheva, O. A.; Strizhakov, R. K.; Rogozhnikova, O. Y.; Troitskaya, T. I.; Fedin, M. V.; Tormyshev, V. M.; Bagryanskaya, E. G. Room-Temperature Tlectron Spin Relaxation of Triarylmethyl Radicals at the X- and Q-Bands. *J. Phys. Chem. B* **2015**, *119* (43), 13630−13640.
(43) Denysenkov, V.; Prandolini, M. J.; Gafurov, M.; Sezer, D.; Endeward, B.; Prisner, T. F. Liquid State DNP Using a 260 GHz High Power Gyrotron. *Phys. Chem. Chem. Phys.* **2010**, *12* (22), 5786−5790.
(44) Denysenkov, V.; Dai, D.; Prisner, T. F. A Triple Resonance (e, 1H, 13C) Probehead for Liquid-State DNP Experiments at 9.4 T. *J. Magn. Reson.* **2022**, *337*, 107185.
(45) Mandal, S.; Sigurdsson, S. T. On the Limited Stability of BDPA Radicals. *Chem. - A Eur. J.* **2020**, *26* (33), 7486−7491.
(46) Poncelet, M.; Driesschaert, B. A 13C-Labeled Triarylmethyl Radical as an EPR Spin Probe Highly Sensitive to Molecular Tumbling. *Angew. Chemie - Int. Ed.* **2020**, *59* (38), 16451−16454.

https://doi.org/10.1021/jacs.3c01358
J. Am. Chem. Soc. 2023, 145, 10268−10274

(47) Raiford, D. S.; Fisk, C. L.; Becker, E. D. Calibration of Methanol and Ethylene Glycol Nuclear Magnetic Resonance Thermometers. *Anal. Chem.* **1979**, *51* (12), 2050−2051.
(48) Sun, Y.; Frenkel-Pinter, M.; Liotta, C. L.; Grover, M. A. The PH Dependent Mechanisms of Non-Enzymatic Peptide Bond Cleavage Reactions. *Phys. Chem. Chem. Phys.* **2020**, *22* (1), 107−113.
(49) Kuzhelev, A. A.; Dai, D.; Denysenkov, V.; Kirilyuk, I. A.; Bagryanskaya, E. G.; Prisner, T. F. Influence of Rotational Motion of Nitroxides on Overhauser Dynamic Nuclear Polarization: A Systematic Study at High Magnetic Fields. *J. Phys. Chem. C* **2021**, *125* (46), 25651−25659.
(50) Bowman, M. K.; Mailer, C.; Halpern, H. J. The Solution Conformation of Triarylmethyl Radicals. *J. Magn. Reson.* **2005**, *172* (2), 254−267.
(51) Leblond, J.; Papon, P.; Korringa, J. Stochastic Theory of Dynamic Spin Polarization in Viscous Liquids with Anisotropic Electron-Spin Relaxation. *Phys. Rev. A* **1971**, *4* (4), 1539−1549.
(52) Kintzinger, J. P.; Zeidler, M. D. Nuclear Magnetic Relaxation Study of Glycerol. *Ber. Bunsenges. Phys. Chem.* **1973**, *77* (2), 98−103.

https://doi.org/10.1021/jacs.3c01358
J. Am. Chem. Soc. 2023, 145, 10268−10274